VIP Electrocatalysis Very Important Paper

Deutsche Ausgabe: DOI: 10.1002/ange.201604372
Internationale Ausgabe: DOI: 10.1002/anie.201604372

Rapid Synthesis of Cobalt Nitride Nanowires: Highly Efficient and Low-Cost Catalysts for Oxygen Evolution

*Yongqi Zhang[+], Bo Ouyang[+], Jing Xu, Guichong Jia, Shi Chen, Rajdeep Singh Rawat, and Hong Jin Fan**

Abstract: *Electrochemical splitting of water to produce hydrogen and oxygen is an important process for many energy storage and conversion devices. Developing efficient, durable, low-cost, and earth-abundant electrocatalysts for the oxygen evolution reaction (OER) is of great urgency. To achieve the rapid synthesis of transition-metal nitride nanostructures and improve their electrocatalytic performance, a new strategy has been developed to convert cobalt oxide precursors into cobalt nitride nanowires through N_2 radio frequency plasma treatment. This method requires significantly shorter reaction times (about 1 min) at room temperature compared to conventional high-temperature NH_3 annealing which requires a few hours. The plasma treatment significantly enhances the OER activity, as evidenced by a low overpotential of 290 mV to reach a current density of 10 mA cm^{-2}, a small Tafel slope, and long-term durability in an alkaline electrolyte.*

The oxygen evolution reaction (OER) is one of the key processes for many energy storage and conversion devices, such as hydrogen production from water splitting, regenerative fuel cells, and rechargeable metal–air batteries.[1] The intrinsic thermodynamic "up-hill" reaction require extra potential to drive the water splitting reaction. To increase the reaction rate and decrease the energy consumption, efficient catalysts with low over-potentials are required to boost this process.[2] Although an excellent OER performance has been achieved for noble metal (Ir and Ru) based materials, the relative scarcity and high cost of these metals renders their application for this purpose unsustainable.[3] Thus, a key goal has been to search for new OER catalytic materials with low over-potential, superior stability, and low cost. Transition-metal nitrides have attracted enormous attention as a result of their high chemical stability and electrical conductivity.[4] It has been confirmed that the introduction of N atoms strongly affects the electronic structure of the metal hosts by charge-transfer processes and/or concomitant structural modification.[4b,5] Transition-metal nitrides show excellent catalytic activities in various fields as a result of their distinct electronic structure.[6] For example, nanostructured Co_4N and Ni_3N were synthesized by Wu and co-workers by ammonia gas annealing the metal precursors, with the compounds exhibiting excellent OER performances.[6b,7] We fabricated 3D porous nickel molybdenum nitride exhibiting an excellent hydrogen evolution reaction (HER) performance.[8]

Great progress has been achieved in the fabrication of metal nitrides.[6b] The commonly applied chemical methods, such as annealing oxide precursors in ambient ammonia and using nitro-organic compounds,[9] have drawbacks, such as the use of toxic and environmentally unfriendly nitrogen sources, high temperatures, and long treatment times. Physical methods, such as magnetron sputtering, are not able to produce specific nanostructured materials. It is well accepted that any efficient catalyst must be composed of tailored nanostructures with high specific surface areas, large reaction sites, and sufficient contact area between reactants and catalyst materials.[10] Thus, a key goal is the development of facile, efficient, and environmentally friendly synthetic methods to produce metal nitrides with tailored nanostructures.

Herein, we demonstrate a fast and convenient method based on N_2 radio frequency (RF) plasma treatment to directly convert Co_3O_4 nanowire arrays into cobalt nitride (CoN). Within just one minute at room temperature, the nitridation process is complete while the nanoarray structure is well preserved. The obtained CoN nanowires function as a highly active and stable non-noble OER electrocatalyst with a low overpotential of 290 mV to reach 10 mA cm^{-2} (η_{10}, i.e. the potential required to reach 10 mA cm^{-2}), a small Tafel slope of 70 mV dec^{-1}, and good stability over 30 h in 1 M KOH. This method is generic and can be employed for the synthesis of various metal nitrides with tailored nanostructures for application in a variety of electrochemical processes (for example, batteries, supercapacitors, electrocatalysis).

First, Co_3O_4 nanowire arrays were prepared as previous reported.[11] Then, the obtained Co_3O_4 nanowires were treated under N_2 RF plasma at room temperature for different time periods, specifically 30 s, 1 min, and 3 min, which are denoted as CoN-30 s, CoN-1 min, and CoN-3 min, respectively. The phase and composition of these samples at different synthesis stages were studied by X-ray diffraction (XRD; Figure 1a; see also Figure S1 in the Supporting Information). After the N_2 plasma treatment, the peaks indexed to the CoN phase appear and those peaks for the Co_3O_4 phase become weaker. In the pattern of the CoN-30 s sample, peaks for Co_3O_4 and CoN coexist. The peak

[*] Y. Zhang,[+] J. Xu, G. Jia, S. Chen, Prof. Dr. H. J. Fan
School of Physical and Mathematical Sciences
Nanyang Technological University
Singapore 637371 (Singapore)
E-mail: fanhj@ntu.edu.sg
B. Ouyang,[+] Prof. Dr. R. S. Rawat
National Institute of Education
Nanyang Technological University
Singapore 637616 (Singapore)
[+] These authors contributed equally to this work.

Supporting information for this article can be found under: http://dx.doi.org/10.1002/anie.201604372.

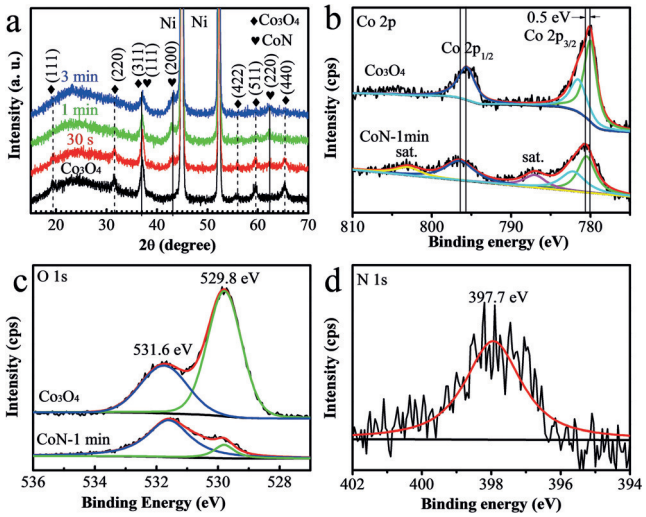

Figure 1. The conversion of Co_3O_4 into CoN. a) XRD patterns of Co_3O_4, CoN-30 s, CoN-1 min, and CoN-3 min. The dashed and solid lines indicate the peak positions of Co_3O_4 and CoN, respectively. b–d) XPS spectra: b) Co 2p spectra of Co_3O_4 and CoN-1 min, c) O 1s spectra of Co_3O_4 and CoN-1 min, d) N 1s spectrum of CoN-1 min.

attributed to the (311) plane of Co_3O_4 and (the 111) plane of CoN overlap at 36.5–36.8°. For the CoN-1 min sample, only peaks indexed to CoN remain (solid line).[12] There is no difference between the pattern of CoN-3 min and that of CoN-1 min, implying that pure CoN nanowire arrays were obtained after just 1 min of N_2 plasma treatment.

The surface chemical states of Co_3O_4 and CoN-1 min were further investigated by X-ray photoelectron spectroscopy (XPS; Figure 1 b–d). For the Co spectra (Figure 1 b), the two dominating peaks, Co $2p_{3/2}$ and Co $2p_{1/2}$, are in good agreement with those reported for Co_3O_4.[13] The relatively weak (negligible) satellite peaks in the XPS spectra of Co_3O_4 confirms its characteristic spinel structure, with Co^{3+} cations occupying octahedral lattice sites and Co^{2+} cations in tetrahedral sites. The emergence of well-defined satellite peaks (at 787.3 and about 803.2 eV) in the CoN-1 min sample is consistent with the breakdown of the spinel structure after nitrogen plasma exposure and the presence of Co^{II}, which indicates the presence of cobalt oxide/hydroxide which is unavoidably formed upon atmospheric exposure.[14] Both peaks of the CoN-1 min sample show a positive chemical shift by 0.5 eV compared with that of Co_3O_4, indicating a modulation of the surface electronic band bending after N_2 plasma. The breakdown of stoichiometric Co_3O_4 after N_2 plasma treatment can also been seen from the O 1s spectra (Figure 1 c). As expected, the intensity of the peak at 531.6 eV, corresponding to surface hydroxy and/or adsorbed oxygen species, has no detectable change after N_2 plasma treatment. In contrast, the peak at 529.8 eV, derived from O^{2-} ions in the crystal lattice of Co_3O_4 or CoO, decreases significantly for the CoN-1 min sample. This corresponds to the stoichiometric breakdown of the Co_3O_4 phase in the CoN-1 min sample along with the conversion into CoN. The smaller but finite intensity of the 529.8 eV peak is due to CoO formation, as was also noticed through the appearance of satellite peaks in the Co 2p spectra (see above). For the N 1s spectrum in Figure 1 d, the broad peak at 397.7 eV is assigned to the nitrogen in a metal nitride environment only for the CoN-1 min sample.[15]

The morphologies of the CoN nanowires at different fabrication stages were examined by using electron microscopy (Figure 2; Figure S2). First, the obtained Co_3O_4 nanowires have a diameter of around 50–100 nm with a tapered morphology (Figure 2 a). SEM images of the CoN-30 s, CoN-1 min, and CoN-3 min samples are presented in Figure S2 c–e. After treatment for 30 s, the nanowire morphology was overall preserved except for a slight twist and granulation of the tips. Increasing the treatment duration to 1 min causes more curvature and entanglement of the nanowires and more evident surface roughness (Figure 2 d). After 3 min plasma treatment, the nanowires are severely etched by nitrogen ions and the array structure no long exists.

Further insights into particle size and morphology of Co_3O_4 and the CoN-1 min sample were obtained from transmission electron microscopy (TEM) images. It can be seen that the Co_3O_4 nanowire is composed of nanoparticles and the edge of nanowire is even (Figure 2 b). The lattice fringes of 0.466 and 0.244 nm determined from Figure 2 c can be assigned to (111) and (311) planes of the spinel Co_3O_4, respectively. After N_2 plasma treatment, the surface of the CoN-1 min nanowire became rougher compared with that of Co_3O_4 (Figure 2 e). The lattice fringes of 0.248 and 0.214 nm in Figure 2 f can be indexed to (111) and (200) planes of the cubic CoN, respectively. These results are in good agreement with the results obtained from XRD measurements.

The catalytic activities of all synthesized materials (Co_3O_4, CoN-30 s, CoN-1 min, and CoN-3 min) for electrochemical water oxidation were evaluated in 1 M KOH solution using a standard three-electrode system (Figure 3). Figure 3 a shows the linear-sweep voltammograms (LSV) at 5 mV s^{-1} after iR correction for all electrodes. It can be seen that the CoN-1 min sample exhibits the highest catalytic activity (highest

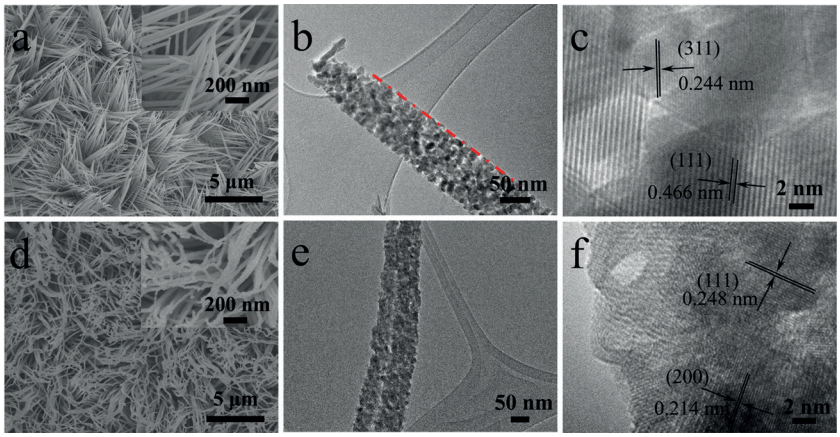

Figure 2. Electron micrographs (SEM and TEM) of pristine Co_3O_4 (a–c) and the CoN-1 min sample (d–f).

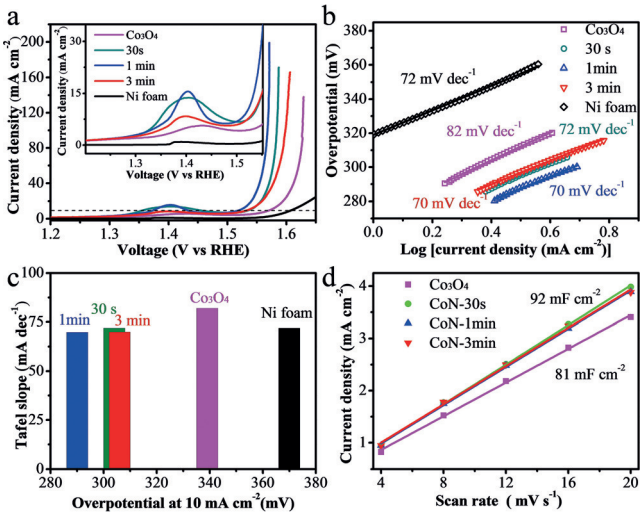

Figure 3. Comparison of the OER performances of different electrodes. a) iR-corrected polarization curves (overpotential versus log of the current density) and b) Tafel plots of Ni foam, Co_3O_4, CoN-30 s, CoN-1 min, and CoN-3 min. c) Comparison of η_{10} values (potentials required to reach 10 mA cm^{-2}) and Tafel slopes for all catalysts. d) Current density as a function of the scan rate for all prepared electrodes, used to indicate the electrochemically active surface area. RHE = reference hydrogen electrode.

levels of current density) across the whole potential window. An overpotential of only 290 mV is required for the CoN-1 min sample to reach a current density of 10 mA cm^{-2} (η_{10}), which is lower than those of Co_3O_4 (339 mV), CoN-30 s (304 mV), and CoN-3 min (306 mV). The Ni foam was also tested for comparison. The poor OER activity of the Ni foam suggests that the high catalytic activity of these samples originates from the CoN nanowires. Moreover, the Tafel slope of the CoN-1 min sample is 70 mV dec^{-1}, smaller than that of Co_3O_4 (82 mV dec^{-1}) and similar to that of CoN-30 s (72 mV dec^{-1}) and CoN-3 min (70 mV dec^{-1}; see Figure 3b). The Tafel slope versus η_{10} value for all of the studied catalysts is plotted in Figure 3c. This comparison shows clearly that the composition conversion of Co_3O_4 into CoN can significantly improve the catalytic activity (larger current density and faster OER rates). We compared our results with previously reported results for Co-related catalysts, such as Co_2B,[14] CoS,[16] CoP_2,[17] and cobalt oxides/hydroxides.[10a,18] Our CoN nanowire arrays obtained by rapid plasma treatment outperform most of the samples in terms of OER catalysis (see Table S1).

The electrochemically active surface areas (EASAs) were estimated by using the electrochemical double-layer capacitance (C_{dl}; Figure 3d, Figure S3). After N_2 plasma treatment, the EASA increased slightly compared with pure Co_3O_4, which may be attributed to the rougher surface achieved during plasma treatment. However, it seems that the EASA does not obviously change when the plasma treatment duration increased from 30 s to 3 min. Therefore, the larger current density of CoN-1 min compared to that of CoN-3 min at the same potential (in Figure 3a) implies that the structure and morphology of the catalyst also play a vital role in catalytic performance. It is known that the quasi-vertical alignment of nanowire arrays is generally favorable for the transport of reactants (H_2O) and products (O_2 and H_2).[10a] The above analyses leads us to the conclusion that the CoN-1 min sample is the most efficient electrocatalyst among the materials investigated herein.

Electrochemical impedance spectroscopy (EIS) was carried out to study the kinetics occurring at the electrode/electrolyte surface under OER conditions. The Nyquist plots in Figure 4a show that the charge-transfer resistance of CoN-1 min decreased significantly in comparison with Co_3O_4. This

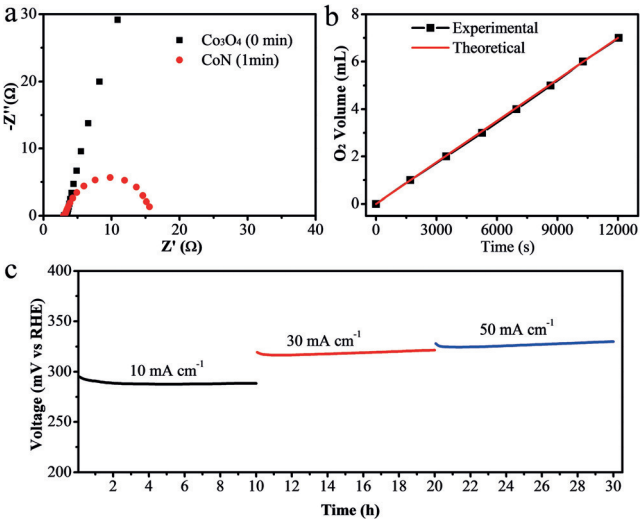

Figure 4. OER performance of the CoN-1 min electrode. a) Nyquist plots of Co_3O_4 and CoN-1 min electrodes (Z″ indicates the imaginary impedance, Z′ is the real impedance). b) Comparison of the evolved oxygen volume with the theoretical oxygen volume calculated based on the amount of consumed charges over the course of electrolysis. c) Stability tests (voltage versus time) of the CoN-1 min catalyst at current densities of 10, 30, and 50 mA cm^{-2} over 30 h.

result suggests that CoN-1 min has the faster charge-transfer process. A Faradaic efficiency measurement at a fixed current density (30 mA cm^{-2}) was carried out to check whether the current was associated with water oxidation (Figure 4b). The Faradaic efficiency was determined by comparing the amount of gas produced experimentally with the theoretically calculated value (see the experimental section in the Support Information for details). The coincidence of both values (near 100% Faradaic efficiency) indicates that no side reaction occurred during electrolysis.

Stability is another important parameter to evaluate an electrocatalyst. To assess the durability of CoN-1 min nanowire arrays for OER in an alkaline electrolyte, electrolysis at three current densities (10, 30, and 50 mA cm^{-2}) was conducted sequentially for over 30 h (Figure 4c). The corresponding overpotential remains stable at around 290, 318, and 325 mV for over 10 h each. The SEM image collected after the 30 h stability test (Figure S4a) shows that the structure of the original nanowire arrays is well preserved. In addition, the C_{dl} value was tested again and there was almost no change after the 30 h electrolysis experiment (Figure S4b,c). These

results indicate that the CoN nanowire arrays are quite stable as OER catalysts.

To better understand the superior performance of the CoN nanowire arrays, the mechanism of catalysis of CoN was studied by cyclic voltammetry (CV), XPS, and TEM after electrolysis (Figure 5). It has been reported that the essentially active sites of non-oxide metal-based catalysts (such as

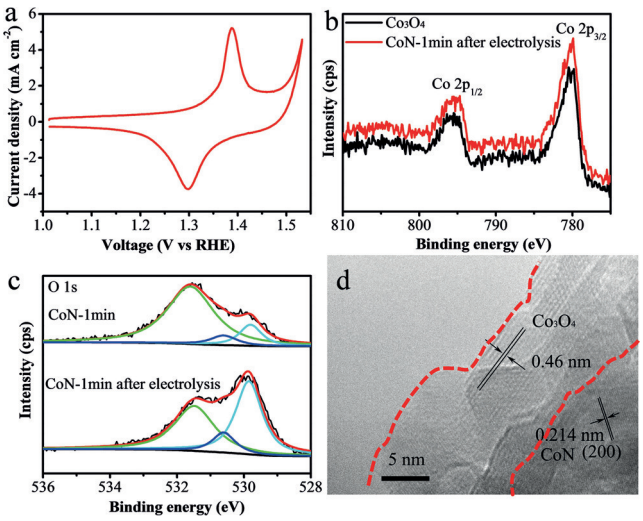

Figure 5. Characterization of the CoN-1 min catalyst. a) Cyclic voltammogram at a scan rate of 1 mv s^{-1}. The XPS b) Co 2p and c) O 1s spectra before and after electrolysis. d) TEM image of the nanowire surface after OER electrolysis.

metal nitrides, phosphides, and borides) for the electrochemical oxidation of water are the thin layer of oxide/hydroxide formed on the surface.[14] In our case, CoN has a similar catalytic mechanism to that proposed above for metal-oxide-based catalysts in alkaline electrolytes. A layer of CoOOH is expected to form on the surface prior to the OER process, which will act as the active site. Next, CoOOH/CoN is further oxidized to form the CoO_2/CoN complex species that is a more efficient species for the OER process. As shown in Figure 5a, the redox waves in the cyclic voltammogram can be attributed to the Co^{3+}/Co^{4+} redox couple. The Co 2p spectrum after electrolysis is similar to that of Co_3O_4, albeit with significantly decreased intensities for satellite peaks but identical binding-energy peak positions, indicating that the Co atoms have the same chemical environment and are in similar oxidation states (Figure 5b). The O 1s XPS spectra in Figure 5c show that the intensity of the peak attributed to oxygen ions in the crystal lattice increases enormously after water electrolysis, in accordance with the proposed formation of cobalt oxide on the surface of CoN nanowire arrays during the electrolysis. The Raman spectra (Figure S4e) also suggested the formation of cobalt oxide. The TEM images of CoN (Figure 5d; Figure S4d) after electrolysis confirmed that a layer of cobalt oxide around 5–10 nm thick formed on the surface of the CoN nanowires.

Finally, the overall water splitting was conducted in a two-electrode configuration by employing the CoN nanowire as the OER electrode and the previously reported porous NiMoN arrays as the HER electrode (Figure S5). Porous NiMoN was synthesized by N_2 plasma treatment of predeposited metal NiMo alloy, and the material was employed as an efficient HER catalyst, achieving a current density of 10 mA cm^{-2} at an overpotential as low as 109 mV.[8] As shown in Figure S5, application of the NiMoN || CoN electrolyzer cell affords a current density of 10 mA cm^{-2} at the operating potential of 1.63 V, representing a combined overpotential of 400 mV for overall water splitting. This voltage is comparable to that of previously reported electrocatalysts in alkaline media (Table S2). More importantly, this combined electrolyzer cell exhibited an excellent stability (see Figure S5c): the operating voltage remained stable at around 1.7 V at a fixed current density of 30 mA cm^{-2} for 120 h of continuous electrolysis. The photograph in Figure S5a shows the obvious production of H_2 and O_2 gas during water electrolysis employing this electrochemical cell configuration.

In summary, we have demonstrated a new and efficient method using N_2 RF plasma to convert cobalt oxide precursors into cobalt nitride with perfect preservation of their nanostructures. This method is environmental friendly, efficient, and safe. As a result of the better conductivity and the preserved large EASA, the obtained CoN nanowire arrays on nickel foam exhibited an outstanding OER performance with a small overpotential of around 290 mV to obtain a current density of 10 mA cm^{-2} and with an outstanding durability at different current densities. The OER performance of the CoN nanowire arrays confirm that metal nitrides are a class of promising noble-metal-free catalysts. To complement the various techniques employed to obtain a large diversity of nanostructured metal oxides, the new method presented in this study may be extended for the fabrication of a wide range of metal nitrides with tailored nanostructures.

Acknowledgements

This work is supported by the Singapore MOE AcRF Tier 1 grant (RG98/15) and NIE AcRF RS 6/14 RSR. It is also partly supported by the Foundation of State Key laboratory of Coal Conversion (Grant No. J16-17-909).

Keywords: cobalt nitride · electrocatalysis · nanostructures · oxygen evolution · water splitting

How to cite: *Angew. Chem. Int. Ed.* **2016**, *55*, 8670–8674
Angew. Chem. **2016**, *128*, 8812–8816

[1] a) J. Suntivich, K. J. May, H. A. Gasteiger, J. B. Goodenough, Y. Shao-Horn, *Science* **2011**, *334*, 1383–1385; b) I. C. Man, H.-Y. Su, F. Calle-Vallejo, H. A. Hansen, J. I. Martínez, N. G. Inoglu, J. Kitchin, T. F. Jaramillo, J. K. Nørskov, J. Rossmeisl, *ChemCatChem* **2011**, *3*, 1159–1165.

[2] a) J. Wang, W. Cui, Q. Liu, Z. Xing, A. M. Asiri, X. Sun, *Adv. Mater.* **2016**, *28*, 215–230; b) J. Wang, H. X. Zhong, Y. L. Qin, X. B. Zhang, *Angew. Chem. Int. Ed.* **2013**, *52*, 5248–5253; *Angew. Chem.* **2013**, *125*, 5356–5361.

[3] a) X. Lu, C. Zhao, *Nat. Commun.* **2015**, *6*, 6616; b) Z. Shan, P. S. Archana, G. Shen, A. Gupta, M. G. Bakker, S. Pan, *J. Am. Chem. Soc.* **2015**, *137*, 11996 – 12005.
[4] a) Y. Zhong, X. Xia, F. Shi, J. Zhan, J. Tu, H. J. Fan, *Adv. Sci.* **2016**, *3*, DOI: 10.1002/advs.201500286; b) W.-F. Chen, J. T. Muckerman, E. Fujita, *Chem. Commun.* **2013**, *49*, 8896 – 8909; c) D. J. Ham, J. S. Lee, *Energies* **2009**, *2*, 873 – 899.
[5] S. Oyama, *Catal. Today* **1992**, *15*, 179 – 200.
[6] a) J. Xie, S. Li, X. Zhang, J. Zhang, R. Wang, H. Zhang, B. Pan, Y. Xie, *Chem. Sci.* **2014**, *5*, 4615 – 4620; b) P. Z. Chen, K. Xu, Z. W. Fang, Y. Tong, J. C. Wu, X. L. Lu, X. Peng, H. Ding, C. Z. Wu, Y. Xie, *Angew. Chem. Int. Ed.* **2015**, *54*, 14710 – 14714; *Angew. Chem.* **2015**, *127*, 14923 – 14927; c) W. F. Chen, K. Sasaki, C. Ma, A. I. Frenkel, N. Marinkovic, J. T. Muckerman, Y. Zhu, R. R. Adzic, *Angew. Chem. Int. Ed.* **2012**, *51*, 6131 – 6135; *Angew. Chem.* **2012**, *124*, 6235 – 6239; d) M. Shalom, D. Ressnig, X. Yang, G. Clavel, T. P. Fellinger, M. Antonietti, *J. Mater. Chem. A* **2015**, *3*, 8171 – 8177.
[7] K. Xu, P. Chen, X. Li, Y. Tong, H. Ding, X. Wu, W. Chu, Z. Peng, C. Wu, Y. Xie, *J. Am. Chem. Soc.* **2015**, *137*, 4119 – 4125.
[8] Y. Zhang, B. Ouyang, J. Xu, S. Chen, R. S. Rawat, H. J. Fan, *Adv. Energy Mater.* **2016**, DOI: 10.1002/aenm.201600221.
[9] M. Shalom, V. Molinari, D. Esposito, G. Clavel, D. Ressnig, C. Giordano, M. Antonietti, *Adv. Mater.* **2014**, *26*, 1272 – 1276.
[10] a) R. Chen, H.-Y. Wang, J. Miao, H. Yang, B. Liu, *Nano Energy* **2015**, *11*, 333 – 340; b) H. B. Wu, B. Y. Xia, L. Yu, X. Y. Yu, X. W. Lou, *Nat. Commun.* **2015**, *6*, 6512.
[11] X. H. Xia, J. P. Tu, Y. Q. Zhang, Y. J. Mai, X. L. Wang, C. D. Gu, X. B. Zhao, *RSC Adv.* **2012**, *2*, 1835 – 1841.
[12] K. Suzuki, T. Kaneko, H. Yoshida, H. Morita, H. Fujimori, *J. Alloys Compd.* **1995**, *224*, 232 – 236.
[13] C. Yan, G. Chen, X. Zhou, J. Sun, C. Lv, *Adv. Funct. Mater.* **2016**, *26*, 1428 – 1436.
[14] J. Masa, P. Weide, D. Peeters, I. Sinev, W. Xia, Z. Sun, C. Somsen, M. Muhler, W. Schuhmann, *Adv. Energy Mater.* **2016**, *6*, DOI: 10.1002/aenm.201502313.
[15] J. Liu, S. Tang, Y. Lu, G. Cai, S. Liang, W. Wang, X. Chen, *Energy Environ. Sci.* **2013**, *6*, 2691 – 2697.
[16] J. Wang, H. X. Zhong, Z. L. Wang, F. L. Meng, X. B. Zhang, *ACS Nano* **2016**, *10*, 2342 – 2348.
[17] Y. P. Zhu, Y. P. Liu, T. Z. Ren, Z. Y. Yuan, *Adv. Funct. Mater.* **2015**, *25*, 7337 – 7347.
[18] S. Li, Y. Wang, S. Peng, L. Zhang, A. M. Al-Enizi, H. Zhang, X. Sun, G. Zheng, *Adv. Energy Mater.* **2016**, *6*, DOI: 10.1002/aenm.201501661.

Received: May 5, 2016
Published online: June 2, 2016

